ISSN 0869-5938, Stratigraphy and Geological Correlation, 2006, Vol. 14, No. 3, pp. 260–274. © MAIK "Nauka/Interperiodica" (Russia), 2006.
Original Russian Text © I.M. Gorokhov, M.A. Semikhatov, M.M. Arakelyants, E.A. Fallick, N.N. Mel'nikov, T.L. Turchenko, T.A. Ivanovskaya, T.S. Zaitseva, E.P. Kutyavin, 2006, published in Stratigrafiya. Geologicheskaya Korrelyatsiya, 2006, Vol. 14, No. 3, pp. 41–56.

Rb–Sr, K–Ar, H- and O-Isotope Systematics of the Middle Riphean Shales from the Debengda Formation, the Olenek Uplift, North Siberia

I. M. Gorokhov[a], M. A. Semikhatov[b], M. M. Arakelyants[c], E. A. Fallick[d], N. N. Mel'nikov[a], T. L. Turchenko[a], T. A. Ivanovskaya[b], T. S. Zaitseva[a], and E. P. Kutyavin[a]

[a] *Institute of Precambrian Geology and Geochronology, Russian Academy of Sciences, St. Petersburg, Russia*
[b] *Geological Institute, Russian Academy of Sciences, Moscow, Russia*
[c] *Institute of Geology of Ore Deposits, Petrography, Mineralogy, and Geochemistry (IGEM), Russian Academy of Sciences, Moscow, Russia*
[d] *Scottish Universities Environmental Research Centre, Glasgow, Scotland*

Received November 25, 2004; in final form, June 29, 2005

Abstract—Clay subfractions (SFs) of <0.1, 0.1–0.2, 0.2–0.3, 0.3–0.6, 0.6–2 and 2–5 μm separated from Middle Riphean shales of the Debengda Formation are studied using the TEM, XRD, K–Ar and Rb–Sr isotopic methods. The oxygen and hydrogen isotope compositions in the SFs are studied as well. The low-temperature illite-smectite is dominant mineral in all the SFs except for the coarsest ones. The XRD, chemical and isotopic data imply that two generations of authigenic illite-smectite different in age are mixed in the SFs. The illite crystallinity index decreases in parallel with size diminishing of clay particles. As compared to coarser SFs, illite of fine-grained subfractions is enriched in Al relative to Fe and Mg, contains more K, and reveals higher K/Rb and Rb/Sr ratios. The Rb–Sr age calculated by means of the leachochron ("inner isochron") method declines gradually from 1254–1272 Ma in the coarsest SFs to 1038–1044 Ma in finest ones, while the K–Ar age decreases simultaneously from 1225–1240 to 1080 Ma. The established positive correlation of $\delta^{18}O$ and δD values with dimensions of clay particles in the SFs seems to be also consistent with the mixing systematics. The isotopic systematics along with data on mineral composition and morphology lead to the conclusion that mixed-layer illite-smectite was formed in the Debengda shales during two periods 1211–1272 and 1038–1080 Ma ago. The first period is likely close to the deposition time of sediments and corresponds to events of burial catagenesis, whereas the second one is correlative with the regional uplift and changes in hydrological regime during the pre-Khaipakh break in sedimentation.

DOI: 10.1134/S0869593806030038

Key words: Proterozoic, Riphean, shales, fine clay fractions, illite-smectite, illite crystallinity index, catagenesis, Rb–Sr age, K–Ar age, oxygen isotope composition, hydrogen isotope composition, systematics of two-component mixing, leaching, North Siberia.

INTRODUCTION

As any shale contains clastic and authigenic mineral phases retaining (or capable to retain) the isotopic memory of diverse events of sedimento- and lithogenesis, it is impossible to use the whole-rock shale samples for the correct dating of sedimentary successions. Isotopic ages obtained for these samples cannot be interpreted confidently in terms of concrete geological events (Clauer, 1976; Bonhomme, 1982; Gorokhov and Semikhatov, 1984; Gorokhov et al., 2003). The idea of isotopic-geochronological and geochemical study of individual minerals from nonmetamorphic clay rocks meets a considerable, often insuperable problem of separating the minerals. The only way to get material enriched in particular clay minerals is to separate different size fractions from a shale sample (Aronson and Hower, 1976; Morton, 1985a, 1985b; Gorokhov et al., 1994, 1997, 2001, 2003).

Many authors who studied Rb–Sr and K–Ar systematics of the fine clay fractions showed that model ages of the latter are getting younger, when clay particles decrease in size (Hower et al., 1963; Hurley et al., 1963; Hofmann et al., 1974; Zhang 1985; Bonhomme, 1987; Mel'nikov et al., 1990; Gorokhov et al., 1994). However, the mineral phases, which originated at particular stages of the rock geological history, can be identified only if the clay fractions studied are in a very narrow (submicron) size range. Morton (1985b) who studied the Rb–Sr systematics using this approach identified two illite polytypes in the Woodford shale of western Texas: one (polytype $2M_1$) derived from provenance and the other one (polytype $1M_d$) formed in the course of the late diagenesis (catagenesis in terminology of

Russian geologists) of original sediment. Following the same approach, Gorokhov et al. (1994) detected in blue clays of northern Estonia three illite generations different in age: detrital ($2M_1$) and two authigenic (1M and $1M_d$). The Rb–Sr age for one of these authigenic generations was close to the timing of sedimentation. It is reasonable to mention one more example when the Rb–Sr age close to stratigraphic one has been obtained by means of analyzing fine-grained clay fractions of shales from the Lower Riphean Ust-Il'ya Formation of the Anabar massif. In this case, procedure of dating included the stage of leaching the separated fine-grained subfractions to plot then "inner isochrons" (Gorokhov et al., 1997).

To use such an approach in practical geochronology, we should know of course to what extent the illite formation is typical of the early burial stages of clay sediments. In this work, we consider this problem using as an example the Middle Riphean shales of the Debengda Formation, the Olenek Uplift, North Siberia. In distinction from our earlier publications dedicated to this problem (Gorokhov et al., 1997, 2001, 2002, 2003), investigation of the Rb–Sr and K–Ar systematics is supplemented here by analysis of hydrogen and oxygen isotopic system in the minerals.

STRATIGRAPHY, AGE LIMITS AND STRUCTURE OF THE DEBENGDA FORMATION

Riphean deposits of the Olenek Uplift, which belong to basal horizons of sedimentary cover in northeastern areas of the Siberian platform, form a gently dipping (commonly 3–5°) monocline complicated by a network of faults (Komar, 1966; Shpunt et al., 1979, 1982). These deposits rest with angular unconformity on the pre-Riphean (older than 1.9 Ga) metamorphic rocks and granitoids of the platform basement, being overlapped transgressively by predominantly carbonate strata of the Vendian. The upper carbonate strata contain fossils characteristic of both zones of the Nemakit-Daldynian Stage (Khomentovskii and Karlova, 2002) and volcanogenic zircons, which yielded the Pb–Pb age of 543.9 ± 0.2 Ma (SHRIMP, Bowring et al., 1993). Judging from data of C-isotope chemostratigraphy, these strata correspond to upper horizons of the Vendian (Semikhatov et al., 2004).

Riphean deposits of the study region (Fig. 1) are divided into six formations (Shpunt et al., 1979, 1982; Shenfil', 1991). These are the Osorkhayata (130 m) and Sygynakhtakh (130–150 m) siliciclastic formations separated by an erosion surface. The Kyutingda Formation (220–260 m) of predominantly carbonate sediments conformably rests on the latter being overlain after a hiatus by the Arymass Formation (170–200 m) of carbonate and siliciclastic rocks. The next Debengda Formation (540–560 m) of siliciclastic and carbonate deposits is bounded from below and at the top by erosion surfaces. Finally, the Khaipakh Formation (200–240 m) that terminates the succession is divided into

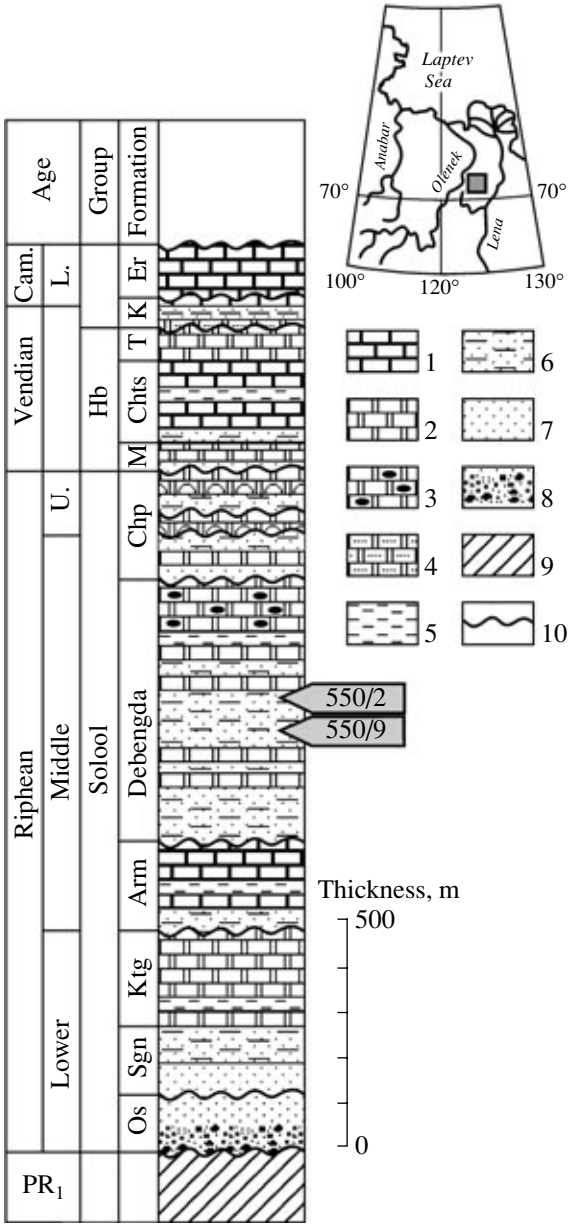

Fig. 1. Lithostratigraphic column of Upper Precambrian sediments with indicated sampling levels and locality of the Olenek Uplift shown in the inset map: (1) limestone; (2) dolostone; (3) dolostone with chert lenses and nodules; (4) sandy dolostone; (5) shale; (6) intercalated shales, siltstones and sandstones; (7) sandstone; (8) gravelstone; (9) crystalline rocks of pre-Riphean basement; (10) erosion surface. Abbreviations: (Cam.) Cambrian; (L) Lower; (U) Upper; (Hb) Khorbusuonka; (Os) Osorkhayata; (Sgn) Sygynakhtakh; (Ktg) Kyutingda; (Arm) Arymass; (Chp) Khaipakh; (M) Maastakh; (Chts) Khatyspyt; (T) Turkut; (K) Kesyussya; (Er) Erkeket

three siliciclastic–carbonate subformations separated by erosion surfaces (Fig. 1). Among five subformations distinguished in the Debengda Formation (Shenfil' et al., 1988; Shenfil', 1991; Gorokhov et al., 1995a), the basal one (115–120 m) is composed of diverse gray siliciclas-

tic rocks with rare intercalations of stromatolitic limestones. In the second subformation (80–85 m), three members of gray stromatolitic limestones are separated by beds of greenish gray sandstones and shales of insignificant thickness. The third subformation is composed of greenish gray siltstones and shales that have been sampled and studied in this work. Brown stromatolitic limestones with thin (1–8 m) intercalations of shales, siltstones and sandstones correspond to the fourth subformation (90–100 m). The fifth subformation (120–150 m) is represented by gray and pink stromatolitic dolostones with cherty lenses and rare interlayers of shales and occasional siltstones. Like siliciclastic rocks of the Osorkhayata, Kyutingda, Arymass and Khaipakh formations, sandstones and siltstones of the Debengda Formation and limestones of its second subformation are enriched to variable extent in globular glauconite.

The Riphean succession of the Olenek Uplift is interpreted in chronometric aspect based on successive stromatolite assemblages (Komar, 1966; Shpunt et al., 1979, 1982; Semikhatov and Serebryakov, 1983) and on K–Ar dates for glauconites. The dates mostly obtained in the 1960s for mineralogically unstudied globules of glauconite–illite composition (Kazakov et al., 1965; Geochronology…, 1968 and references therein) represent the following series of values declining upward in the succession: 1435 Ma in the Sygynakhtakh Formation; 1350 Ma in the Kyutingda Formation; 1220–1165 Ma in the Arymass Formation; 1135, 1080 and 1040 Ma in the lower, middle and upper parts of the Debengda Formation; 1000 and 960 Ma in the lower part of the Khaipakh Formation. Since information about composition and structure of the studied mineral geochronometers is unavailable, the dates can be considered now as tentative only. The concordant Rb–Sr isochron and K–Ar age values of 1262 ± 13 and 1287 ± 16 Ma (Gorokhov et al., 1995a) represent the most confident geochronological assessments for two lower subformations of the Debengda Formation. They characterize well-studied large globules of glauconite and Al-glauconite, which are very dense and colored green regardless of their composition and contain 6.3 to 6.7% of potassium and less than 20% of smectite layers. According to Mössbauer spectra, these glauconites were not subjected to secondary alterations that could result in radiogenic ^{87}Sr and ^{40}Ar loss (Gorokhov et al., 1995a; Zaitseva et al., 2004). Besides, Ponomarchuk et al. (1994) published K–Ar dates for whole-rock carbonate samples from Riphean succession of the Olenek Uplift, but these dates can hardly be connected with real events known in the geological history of the region, because K-bearing mineral phases have not been identified in the analyzed rocks.

Among successive stromatolite assemblages known from the Riphean succession of the Olenek Uplift, the oldest one is detected in the Kyutingda Formation (Komar, 1966; Shpunt et al., 1979, 1982). In the formation lower part, there was found *Kussiella kussiensis*, the passively branching species typical of the Lower Riphean and occurring in association with Siberian endemics and columnar stromatolites of wide stratigraphic ranges. In the formation upper part, these stromatolites are replaced by assemblage of stratal form species representing the endemic stromatolite morphotypes of North Siberia. These successive assemblages and lithologic data suggest that the Kyutingda Formation of the Olenek Uplift is correlative with the Ust-Il'ya and Kotuikan formations of the Anabar massif (Komar, 1966; Shpunt et al., 1979, 1982; Semikhatov and Serebryakov, 1983; Shenfil', 1991). The established correlation is important, because the early diagenesis of the Ust-Il'ya sediments took place 1483 ± 10 or 1459 ± 20 Ma ago, as is estimated based on Rb–Sr and K–Ar dates obtained for glauconite. On the other hand, burial diagenesis (catagenesis) of sediments happened 1405–1415 Ma ago according to Rb–Sr dates for a series of clay-size fractions from shales (Gorokhov et al., 1991, 1997).

A complete renewal of stromatolite assemblages is recorded in the Arymass Formation. Abundant *Baicalia, Conophyton lituus* and *Jacutophyton multiforme* occurring here are characteristic of the Middle and lower Upper Riphean. They occur as well in overlying Debengda and lower Khaipakh deposits, being associated at these levels with some taxa known only from North Siberia (Semikhatov, 1985) and with *Conophyton metula* and *Jacutophyton cognitum*, which appear in the Middle Riphean. Another level, where the complete renewal of stromatolite assemblages is recorded, has been detected at the base of the second Khaipakh Subformation. All the taxa listed above disappear here to be replaced by a new assemblage including the following morphotypes: *Inzeria tjomusi* and *Jurusania cylindrica* characteristic of the lower Upper Riphean, the form genus *Gymnosolen* typical of the Upper Riphean, and some endemic stromatolites. In addition to North Siberian endemics, the upper Khaipakh deposits contain local representatives of the genus *Boxonia* that is widespread in the Upper Riphean and Vendian.

According to data presented above, the Lower–Middle Riphean boundary separates the Kyutingda and Arymass formations, whereas the Middle–Upper Riphean boundary is detectable between the first and second subformations of the Khaipakh Formation (Shpunt et al., 1979, 1982; Gorokhov et al., 1995a). Consequently, the Debengda Formation spans the middle and upper parts of the Middle Riphean that has chronometric range from 1350 ± 20 to 1030 ± 30 Ma (Semikhatov et al., 1991; Semikhatov, 2000). The inferred range of the Debengda Formation is consistent with data on composition of silicified microfossils from its rocks (Sergeev et al., 1994) and with appearance of organic-walled acanthomorphic acritarchs *Trachyhystrichosphera vidalii* (Vidal et al., 1993), which are typical of the Upper Riphean, in the upper Khaipakh strata. However, some researchers attribute the Debengda Formation to the Upper Riphean. On the one hand, this opinion has been argued for by adherents of the peculiar event

model of the Upper Riphean base (Khomentovskii et al., 1985; Shenfil' et al., 1988; Shenfil', 1991; Khomentovskii, 1996), which differs from that authorized in the General stratigraphic scale (Semikhatov et al., 1991). On the other hand, it has been thought that carbonaceous fossils *Chuaria circularis* and *Tawuia dalensis*, which occur in the Debengda Formation, appear in geological record since the Late Riphean only (Vidal et al., 1993). Beyond North Siberia however, these fossils occur undoubtedly below the Upper Riphean (Hofmann, 1992, and references therein). Thus, we believe that position of shales, which have been sampled from the third subformation of the Debengda Formation and studied in this work, is close to the base of the upper third of the Middle Riphean succession in the Olenek Uplift.

According to thickness of post-Debengda deposits in the Olenek Uplift and flanking structures, the Debengda shales have never been buried deeper than 4–5 km in the course of geological evolution. Color index of organic-walled microfossils (Hayes et al., 1983) from the least altered shales of the formation (unpublished data of A.F. Veis) also suggests that the rocks have never been heated above 80°C. As is evident from mineralogical studies, sediments of two lower Debengda subformations (outside contact zones around basic sills) have been altered under conditions of deep and retrogressive catagenesis (Ivanovskaya, 1994; Gorokhov et al., 1995a).

INVESTIGATION METHODS

Two samples (nos. 550/2 and 550/9, 250 to 300 g in weight) of greenish gray and gray shales, which have been sampled in the middle of the third Debengda Subformation (Fig. 1) and studied, are lacking obvious signs of secondary alterations. The rocks contain insignificant silty admixture, framboidal pyrite, rare biogenic films, and fine dispersed organic matter. Being cleaned of surficial weathering material, the samples have been comminuted in a hand-power press into powder so that the whole material can pass through the sieve <0.25 mm. A weighing of about 40 g was mechanically mixed in distilled water during 30 minutes to get a suspension and to separate fraction <5 μm from the latter by means of sedimentation technique. The subsequent centrifuging and ultrafiltration was applied to split the latter fraction into granulometric subfractions (SFs) with equivalent spherical diameters of particles <0.1, 0.1–0.2, 0.2–0.3, 0.3–0.6, 0.6–2, and 2–5 μm. Each SF obtained was a few hundreds mg in weight.

Diffractometer DRON UM-1 (filtered CoK_α radiation) was used to study mineral composition of the SFs in oriented slides and to measure the illite crystallinity index I_k (Kubler, 1966, 1990), the width of 10 Å peak at its half height, and ratio of 5 Å- and 10 Å peaks (I_{002}/I_{001}). The illite polytypes were identified based on oblique texture electron diffraction data. Morphology of clay particles was studied in suspension mounted on carbon-covered grid under transmission electron microscope JEM-100B at the Analytical Center MEKHANOBR (St. Petersburg) by magnification 15000 to 40000.

Procedure of the SFs leaching in 1N solution of ammonium acetate has been used to study the Rb–Sr systematics. The procedure is aimed at separation of Sr fixed in the structure of clay minerals from Sr residing in exchangeable positions, adsorbed onto surface of mineral grains, or captured by authigenic carbonates and phosphates. The SF batch subjected to leaching was 60 to 100 mg depending on amount of available material. Residues separated from leachates by centrifuging were washed twice in the bidistilled water, and washing water was added to leachates. All the leachates, residues, and untreated SFs were studied by the Rb–Sr method. The $^{87}Rb/^{86}Sr$ and $^{87}Sr/^{86}Sr$ ratios were determined by isotope dilution method using mixed $^{87}Rb/^{84}Sr$ spike. After dissolution of SFs in the mixture of distilled concentrated HF and H_2SO_4, Rb and Sr were extracted using the ion-exchange column containing Dowex AG50W × 8 (200–400 mesh) resin and 2.5N HCl as an eluent. The Sr isotopic composition was analyzed in static mode on Finnigan MAT 261 multicollector thermal ionization mass spectrometer with Re-filaments. The laboratory average of $^{87}Sr/^{86}Sr = 0.710259 \pm 0.000012$ ($2\sigma_{mean}$, $n = 15$) was determined for the NIST SRM-987 standard carbonate during the period of data gathering. The $^{85}Rb/^{87}Rb$ ratio is measured on MI 1320 20 cm radius, 90° sector, single-collector mass spectrometer with a triple (Re + W) filament ion source. The total processing blank for Sr was less than 5 ng. During the period of data gathering, the average Rb and Sr concentrations of 522 and 65.6 mg/g, respectively, were determined for the NIST 70a K-feldspar. The analytical uncertainty for $^{87}Rb/^{86}Sr$ ratio in SFs is established at ±1%, and that for $^{87}Sr/^{86}Sr$ ratio is estimated at 0.1%. The regression approach of McIntyre et al. (1966) was used to determine the leachochron ("inner isochron") parameters based on the data points characterizing leachate, residue, and untreated material of SFs, and statistical estimation of regression parameters was made by Williamson's method (Williamson, 1968).

The K concentrations are measured by isotope dilution mass spectrometry using ^{41}K spike. The given SF batch (ca. 0.02 g) was subjected to dissolution in a Teflon container with a mixture of concentrated HF + HCl + HNO_3 + $HClO_4$ during 48 hours under room temperature. Residue after evaporation was dissolved in concentrated HNO_3 and HCl to be converted then into chloride. The ion-exchange method on AG50W × 8 (200–400 mesh) resin in H^+ form was used to extract K with 2.4N HCl eluent. The eluted fraction dried completely by heating was converted into sulfate in concentrated H_2SO_4. The K isotope composition was analyzed on MI 1320 single-collector mass spectrometer. To control correctness of analytical results, we analyzed dur-

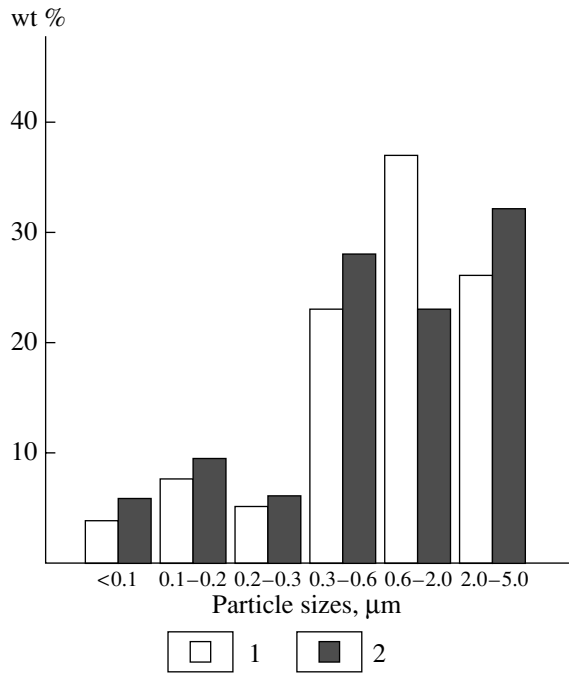

Fig. 2. Distribution histogram of size subfractions in clay fractions <5 μm from samples 550/2 (1) and 550/9 (2).

ing experiments the standard muscovite P-207, biotite LP-6, and biotite 70 samples. The average K contents determined for these standards correspond to 8.68, 8.44 and 7.82%, respectively; precision of the values obtained is ±3%.

Concentration of radiogenic ^{40}Ar in the SFs was measured by isotope dilution technique with ^{38}Ar tracer, using a specialized composite equipment assembled with MI 1201 IG mass spectrometer. The equipment sensitivity to argon is 5×10^{-3} A/torr, and the total processing blank is 5×10^{-10} cm^3 under standard conditions. Isotopic composition of the atmospheric argon and minor batches (ca. 4 mg) of standard biotite Bern 4B, muscovite Bern 4M and muscovite P-207 samples were analyzed to control precision and accuracy of measurements. The radiogenic ^{40}Ar content measured in the above standards corresponds to 9.39, 11,44 and 50.70 ng/g, respectively.

Table 1. XRD characteristics of illite in clay subfractions

Subfraction, μm	Crystallinity index, I_k		Ratio I_{002}/I_{001}
	sample 550/2	sample 550/9	sample 550/9
2–5	n.d.	n.d.	0.20
0.6–2	1.65	1.52	0.21
0.3–0.6	1.54	1.50	0.28
0.2–0.3	1.47	1.49	0.32
0.1–0.2	1.39	1.44	0.55
<0.1	1.26	1.38	0.34

$\delta^{18}O$ was determined by a modified version (see Macaulay et al., 2000) of the laser-fluorination technique described by Sharp (1990). The method involved complete reaction of ca. 1 mg of mineral separate with chlorine trifluoride whilst being heated with a CO_2 laser. The released oxygen was passed through an in-line Hg diffusion pump before conversion to CO_2 on platinized graphite. The reaction yield was measured by capacitance manometer. The gas handling system was on-line to a dedicated VG PRISM 3 dual inlet isotope ratio mass spectrometer. Precision and accuracy on quartz standards are ±0.4‰ (2σ), but for fine-grained hydrous phyllosilicates, the precision was somewhat lower, perhaps 0.6‰. The water content and δD were determined by *in vaccuo* dehydroxylation of ca. 60 mg of mineral separate in a previously degassed platinum crucible that was heated by induction to above 1200°C (see Fallick et al., 1993). The released water was purified and then converted to hydrogen over hot uranium (Bigeleisen et al., 1952). Prior to dehydroxylation, the sample was heated *in vaccuo* overnight at 120°C to reduce the influence of surface-held water. The hydrogen yield (expressed as H_2O^+μmoles/mg) was measured manometrically, and δD value was determined on VG 602 dual inlet mass spectrometer. The NIST 28 biotite gives δD = –65‰ by this method with a precision of ±4‰. For the samples studied here, the precision was probably better than ±10‰. All isotope data characterizing the SFs are presented in per mile notation relative to Vienna Standard Mean Ocean Water (V-SMOW).

Decay constants used to calculate Rb–Sr and K–Ar age are as follows: $\lambda^{87}Rb = 1.42 \times 10^{-11}$ year^{-1}; $\lambda_K = 0.581 \times 10^{-10}$ year^{-1}; $\lambda_\beta = 4.962 \times 10^{-10}$ year^{-1}; $^{40}K = 0.01167$ at %. All uncertainties in this work are quotes at the 2σ level.

RESULTS AND DISCUSSION

Three SFs with particle sizes more than 0.6 μm represent 80 to 85% in <5μm clay separates of both samples studied (Fig. 2). The XRD study showed that all the SFs are dominated by illite-smectite, containing not more than 5% of chlorite. Approximately equal percentages of illite-smectite, chlorite and quartz are established in the SFs 2–5μm. High values of illite crystallinity index (I_k), which characterize genesis of minerals in the diagenesis/catagenesis zone (Kisch, 1980), are established for both samples. In Sample 550/2, I_k decreases from 1.65° in the SF 0.6–2 μm to 1.26° in the SF <0.1 μm; in Sample 550/9 it decreases from 1.52 to 1.38° (Table 1). In the finest SFs (<0.1 and 0.1–0.2μm), illite structure is more ordered (polytype 1M–1M_d) than in coarser separates containing polytype 1M_d. The I_{002}/I_{001} ratio grows in Sample 550/9 from 0.20 (SF 2–5 μm) to 0.55 (SF 0.1–0.2 μm) and then declines down to 0.34 in the SF <0.1 μm (Table 1). This ratio has been considered as indicative of Al abundance in octahedral illite layers relative to Fe + Mg (Esquevin,

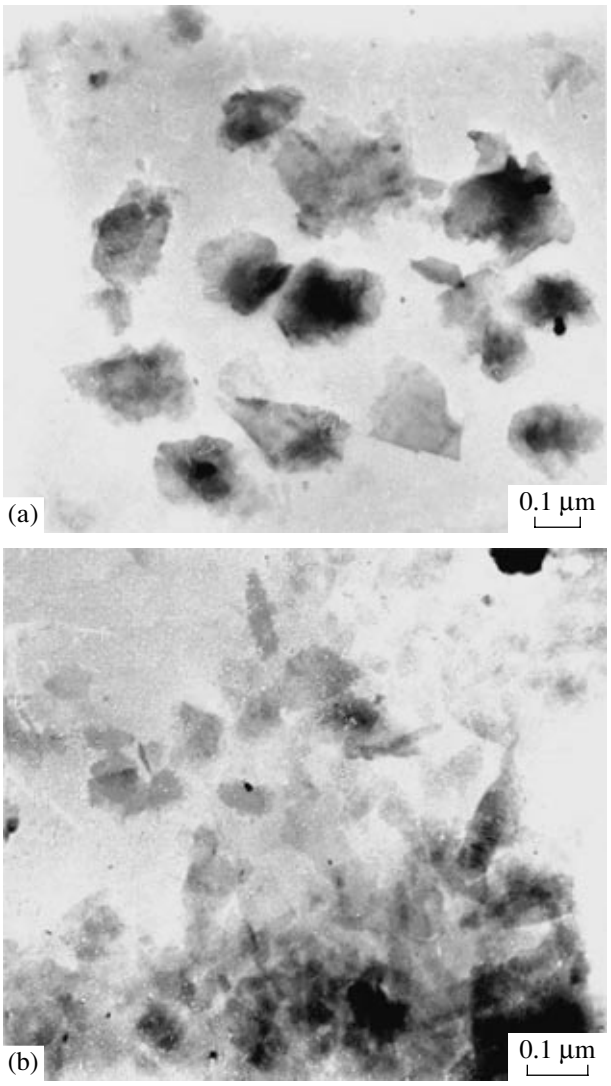

Fig. 3. Microphotographs of clay particles from Sample 550/9 analyzed by transmission electron microscopy: (a) subfraction 0.2–0.3 μm; (b) subfraction <0.1 μm.

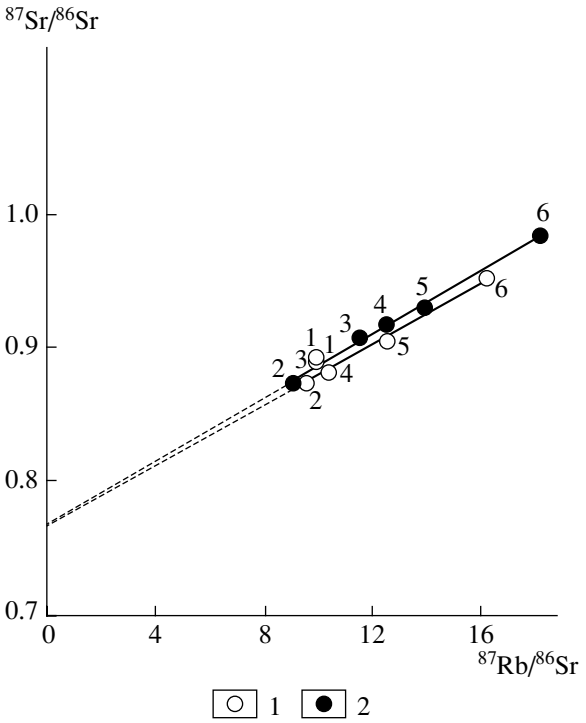

Fig. 4. Rb–Sr diagram for residues of clay subfractions from samples 550/2 (1) and 550/9 (2) after leaching experiments; dots numbered in diagram denote subfractions 2–5 (1), 0.6–2 (2), 0.3–0.6 (3) 0.2–0.3 (4), 0.1–0.2 (5) and <0.1 (6) μm.

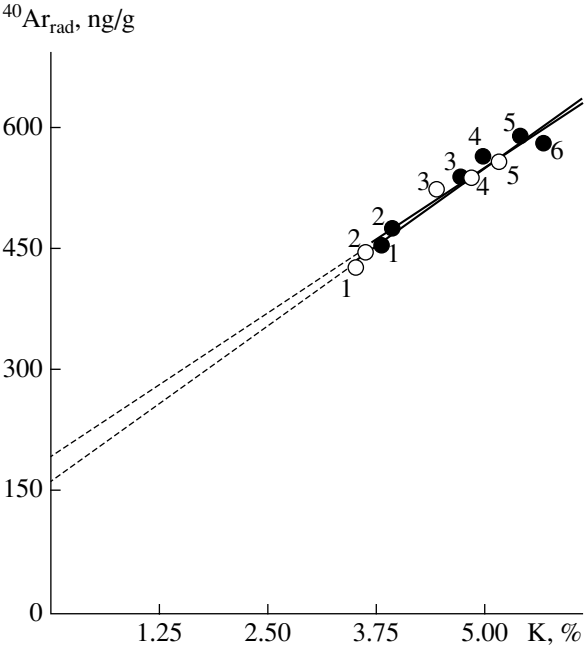

Fig. 5. K–Ar diagram for clay subfractions of samples 550/2 (I) and 550/9 (II); size ranges of subfractions are numbered as in Fig. 4

1969; Środoń and Eberl, 1984). The above data imply therefore that Al is relatively more concentrated in the fine-grained SFs as compared to coarser ones.

Illite particles are of a rather uniform morphology in all the SFs (Fig. 3). Large isometric nepheloid particles have diffuse margins. In addition to nepheloid particles, the finest SFs (<0.1 μm) contain lath-like illite microcrystals with uneven to serrate lateral sides.

The Rb–Sr, K–Ar, oxygen and hydrogen isotopic data characterizing clay material of shales are presented in Tables 2–4. Except for the SF 2–5 μm, all isotopic parameters are dependent on particle sizes. In both SF series for instance, percentage of leachable Sr gradually increases from 47–54 to 66–73%, when particle sizes decrease from 0.6–2 to <0.1 μm, while the $^{87}Rb/^{86}Sr$ ratio in the residues is similarly getting higher

Table 2. Rb–Sr analytical data

Particle size, μm	Type of substance*	Leachable, %		Rb**, ppm	Sr**, ppm	$^{87}Rb/^{86}Sr$	$^{87}Sr/^{86}Sr$
		Rb	Sr				
Sample 550/2							
2–5	U			191	125	4.471	0.79379
	L	1.2	55.0	2.34	68.8	0.0984	0.71378
	R			186	55.4	9.881	0.89195
0.6–2	U			198	141	4.077	0.78538
	L	0.8	54.2	1.58	76.4	0.0599	0.71527
	R			198	64.5	9.034	0.87069
0.3–0.6	U			219	161	3.968	0.78053
	L	1.1	58.3	2.34	93.9	0.0722	0.71535
	R			215	66.6	9.509	0.87408
0.2–0.3	U			234	175	3.891	0.77717
	L	2.0	62.9	4.63	110	0.1225	0.71567
	R			228	64.8	10.35	0.88229
0.1–0.2	U			244	161	4.418	0.78189
	L	1.8	65.2	4.28	105	0.1178	0.71587
	R			238	56.3	12.48	0.90600
<0.1	U			256	171	4.351	0.77826
	L	2.4	73.1	6.18	125	0.1433	0.71552
	R			249	45.8	16.10	0.95248
Sample 550/9							
2–5	U			195	109	5.236	0.80604
	L	2.3	47.1	2.86	51.3	0.1616	0.71489
	R			191	56.8	9.881	0.88983
0.6–2	U			198	121	4.777	0.79728
	L	0.9	46.6	1.83	56.4	0.0941	0.71491
	R			194	63.1	9.026	0.87345
0.3–0.6	U			223	132	4.942	0.79646
	L	1.7	57.0	3.69	75.2	0.1421	0.71527
	R			218	56.0	11.49	0.90832
0.2–0.3	U			233	128	13.30	0.79979
	L	2.3	58.3	5.43	74.6	0.2107	0.71660
	R			225	53.3	12.48	0.91773
0.1–0.2	U			250	134	5.430	0.79793
	L	2.5	61.5	6.29	82.4	0.2209	0.71641
	R			243	51.7	13.91	0.93115
<0.1	U			257	123	6.104	0.80266
	L	2.2	65.9	5.53	81.0	0.1980	0.71561
	R			249	40.9	18.12	0.98445

Notes: * (U) untreated subfraction, (L) acetate leachate, (R) residue after leaching.

** Rb and Sr concentrations in leachates and residues are recalculated for 1 g of untreated subfraction.

from 9.0 to 16.1–18.1 (Table 2). Concentrations of K and ^{40}Ar grow in the same direction from 3.5–3.8 to 5.2–5.6% and from 426–454 to 587 ng/g, whereas the K/Rb ratio increases from 182–194 to 211–220 (Table 3). Parameters $\delta^{18}O$ and δD in the SFs 2–5 and 0.6–2 μm are higher than in finer SFs (Table 4), although the total range of δD variations is just a bit greater than analytical uncertainty.

In the $^{87}Rb/^{86}Sr$–$^{87}Sr/^{86}Sr$ diagram (Fig. 4), data points characterizing residues (discarding SFs 2–5 μm) plot along two linear regression lines. Two regression lines in the diagram K–^{40}Ar (Harper, 1970) can be also regarded as linear to a first approximation, although in fact they are insignificantly curved. Two alternative interpretations are admissible for regression lines observable in the diagrams. On the one hand, the lines may be real age relationships being representative of the illite formation (transformation) at a certain stage of lithogenesis. On the other hand, they may represent mixing lines of two non-cogenetic components with different Rb/Sr ratios and K concentration, thus having no geochronological meaning. A preferable interpretation is of crucial significance for correct understanding of all the results obtained.

The first interpretation is consistent with two facts. First, the regression lines approximating data points of residues in the Rb–Sr diagram (Fig. 4) have similar slopes, which correspond to isochron ages of 807 Ma (Sample 550/2) and 852 Ma (Sample 550/9), and almost identical intercepts on ordinate (0.7646 and 0.7649, respectively). Second, extrapolating quasilinear regressions in Fig. 5 to zero K content and assuming that the ^{40}Ar excess of about 160–190 ng/g is characteristic of all the SFs, we obtain K–Ar ages of 876 and 820 Ma for samples 550/2 and 550/5, respectively. These and apparent Rb–Sr ages quoted above can be regarded as concordant to a first approximation.

Arguments in favor of the second interpretation are as follows. (1) The XRD characteristics of illite depend on particle sizes: in the finest SF (<0.1 μm), illite polytype 1M–$1M_d$ is of a more ordered structure than polytype $1M_d$ prevailing in coarser SFs, and the illite crystallinity index decreases when clay particles diminish in size (Table 1). (2) Chemical composition of illite is variable: in the finer-grained SFs, this mineral is enriched in Al relative to Fe and Mg (Table 1), contains more K (Table 3), and reveals higher K/Rb and Rb/Sr ratios than in coarser SFs (Tables 2 and 3). (3) Isotopic parameters of SFs change as well: in the $1/Sr - {}^{87}Sr/{}^{86}Sr$ diagram (Fig. 6), data points characterizing SFs of both samples, which range in size from 0.3–0.6 to <0.1μm), plot along straight lines matching well the systematics of two-component mixing. Four points characterizing SFs 2–5 and 0.6–2 μm) of both samples deviate from straight lines in Fig. 6 likely because of chlorite present in these SFs and contravening that systematics. Besides, the points of SFs 2–5 μm) plot away from regression lines also in the Rb–Sr diagram (Fig. 4).

Table 3. K-Ar analytical data

Sample	Subfraction, μm	K, %	K/Rb	$^{40}Ar_{rad}$, ng/g	K–Ar age, Ma
550/2	2–5	3.49	182	426.1	1230
	0.6–2	3.60	182	446.2	1240
	0.3–0.6	4.43	202	523.3	1200
	0.2–0.3	4.84	207	539.1	1150
	0.1–0.2	5.15	211	557.1	1125
550/9	2–5	3.78	194	453.9	1215
	0.6–2	3.91	197	474.8	1225
	0.3–0.6	4.71	211	540.2	1175
	0.2–0.3	4.95	212	564.3	1170
	0.1–0.2	5.39	216	586.7	1130
	<0.1	5.65	220	580.8	1080

Table 4. Oxygen and hydrogen isotopic composition in subfractions of Sample 550/9

Subfraction, μm	$\delta^{18}O$ V-SMOW, ‰	δD V-SMOW, ‰	H_2O^+, micromole/mg
2–5	16.7	–87	2.4
	16.6		
0.6–2	15.4	–100	1.4
	15.4		
0.3–0.6	14.3	–94	2.8
	14.5		
0.2–0.3	14.3	–100	2.2
	13.6		
	13.6		
	14.3		
0.1–0.2	14.1	–105	2.6
	14.1		
<0.1	14.0	–108	3.5
	13.5		

(4) Indicative of the mixing systematics could be the other two facts as well: a negative correlation between K concentrations and apparent K–Ar age (Table 3), and dependence of $\delta^{18}O$ and δD values on the particle sizes in SFs of both samples (Table 4).

With regard to the first alternative interpretation, it is necessary to mention an important point. If linear regressions in Figs. 4 and 5 are isochrons, they mean either the origin of illite in the Debengda Formation shales in response to some post-sedimentation event, which took place 810–880 Ma ago, or a complete transformation of the Rb–Sr and K-Ar isotopic systems in clay minerals at that time. In the last case, the Sr isotopic composition had to be homogenized in the samples

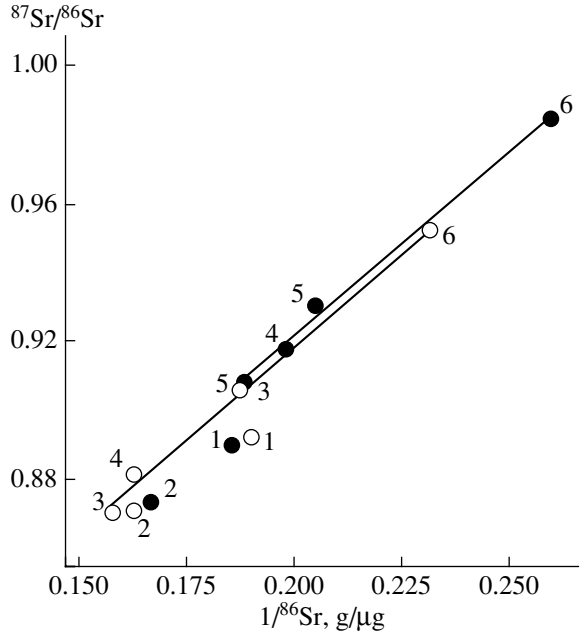

Fig. 6. $^{87}Sr/^{86}Sr$– $1/^{86}Sr$ diagram for residues of clay subfractions after leaching experiment; numbered symbols correspond to those in Fig. 4.

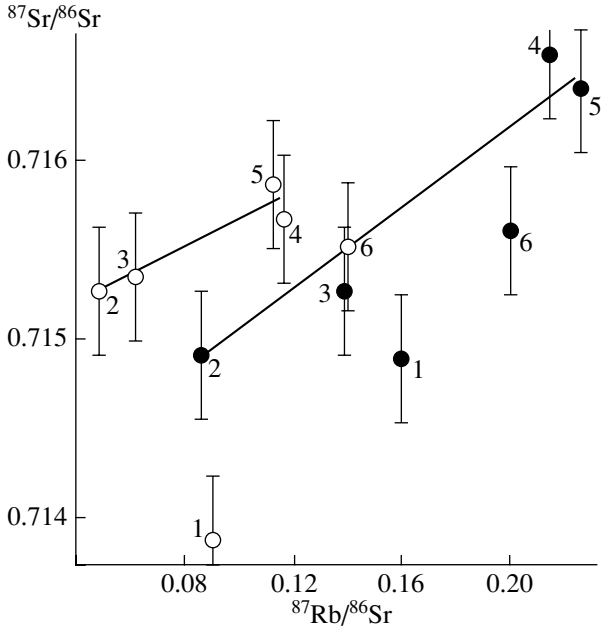

Fig. 7. Rb–Sr diagram for acetate leachates of clay subfractions; numbered symbols correspond to those in Fig. 4.

studied and, perhaps, within the entire horizon of the third subformation, which has been sampled. Moreover, the crystalline structure of illite must captured in both cases a considerable amount of excessive ^{40}Ar.

If illite was formed 810–880 Ma ago, the ^{40}Ar excess and the high $^{87}Sr/^{86}Sr$ ratio in this mineral would mean its origin through dissolution of old clastic material (micas and feldspars) present in the Debengda sediments under condition of a closed or semiclosed geochemical system. Such a situation is typical of the burial catagenesis (Gorokhov et al., 1994; Clauer and Chaudhuri, 1995). With due regard for isotopic ages of glauconites from the Debengda Formation (Rb–Sr date of 1262 ± 13 Ma and K–Ar date of 1287 ± 16 Ma, Gorokhov et al., 1995a), it is difficult to admit however that deposition and burial of sediments were separated by a time span 400 m.y. long. This was hardly probable, because thick sedimentary successions accumulated after deposition of the Debengda sediments are unknown in the study region. On the other hand, the presumable homogenization of Sr isotopic composition in illites existed prior to 810–880 Ma ago seems unlikely in view of equal amounts of ^{40}Ar captured by illite particles different in size, if there was no complete recrystallization of fine clay material in the Debengda sediments. Consequently, if linear regressions in Figs. 4 and 5 are admitted to be isochrons, one must expect unavoidably that clay minerals of shales have been completely recrystallized in equilibrium with pore fluids.

Equilibrium recrystallization of this kind is inconsistent with peculiarities in structure and chemical composition of illites separated from the Debengda shales, primarily with degree of ordering in illite and illite polytypes present in the SFs of different size ranges. Deserving attention here is the more ordered structure of illite prevailing in the fine-grained SFs as compared to coarser illite flakes, i.e., the situation contrasting to that typical of many other Upper Proterozoic clay rocks described earlier (Gorokhov et al., 1994, 1995, 2001, 2002). The idea of one-stage illite recrystallization is equally inconsistent with data on chemical composition, especially on the Rb/Sr ratios characterizing this mineral from SFs of different size ranges. In the case of one illite generation, one should expect the higher Rb/Sr ratios in larger crystals ("Ostwald ripening," Eberl et al., 1990) rather than in smaller ones, as is established for the Debengda shales.

Variations of $\delta^{18}O$ and δD values characterizing different size SFs represent an obvious argument against the one-stage equilibrium recrystallization of illite. As is known (Hoefs, 1980), fractionation of oxygen and hydrogen isotopes is controlled, besides the other factors, by cations they are linked with. In particular, the heavy oxygen isotope tends to be concentrated in layered silicates enriched in Al rather than in Fe. Lawrence and Taylor (1972) showed that $\delta^{18}O$ is by 2–3‰ higher in smectite depleted in Fe than in Fe-smectite. As is shown in the other series of works (Taylor and Epstein, 1966; Suzuoki and Epstein, 1976; Kuroda et al., 1976; Brigham and O'Neil, 1985; Sheppard and Glig, 1996), cations of hydrous silicates influence as well the hydrogen isotope fractionation, and deuterium tends to be concentrated in minerals with prevailing Al–OH ionic

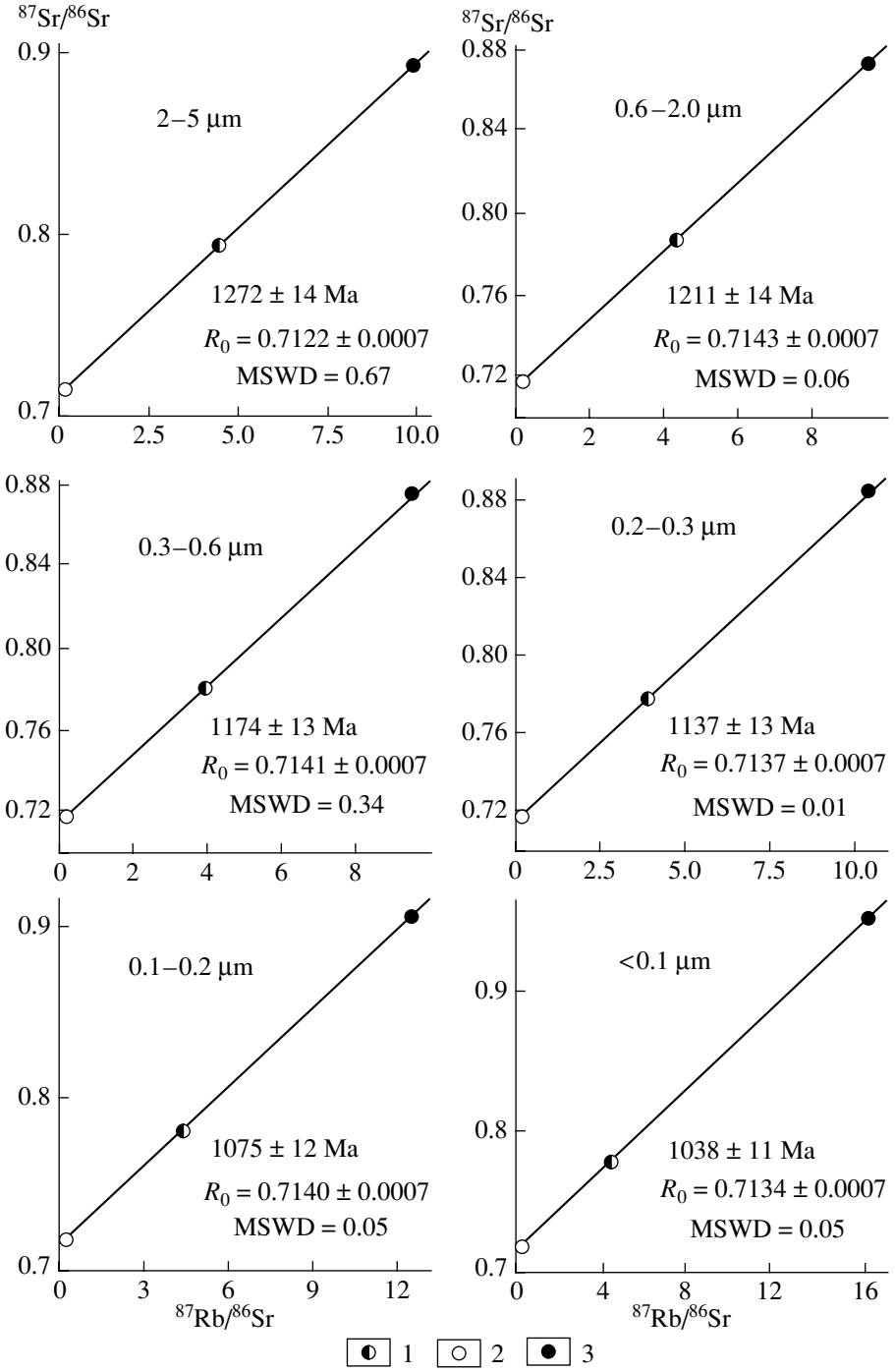

Fig. 8. Inner Rb–Sr isochrons plotted for untreated subfractions (1), acetate leachates (2) and residues after leaching (3), Sample 550/2.

bonds. Accordingly, δD tend to be greater in layered silicates with higher Al/Fe ratio in their octahedral layers, and muscovite always contain more deuterium than paragenetic biotite. At the same time, the isotopic fractionation dependent on difference in crystalline structures of minerals is commonly less significant than effects resulting from changes in their chemical composition.

Turning now to data of Table 4, we can easily see exactly the counter trends of $\delta^{18}O$ and δD variations in different SFs of Sample 550/9 as compared to the trends expectable in the case of one-stage equilibrium recrystallization of illite material. In the finest SFs (<0.1 and 0.1–0.2 μm) containing much illite enriched in Al, $\delta^{18}O$ and δD are at the minimum in contrast to high values, which could be expected in the case of

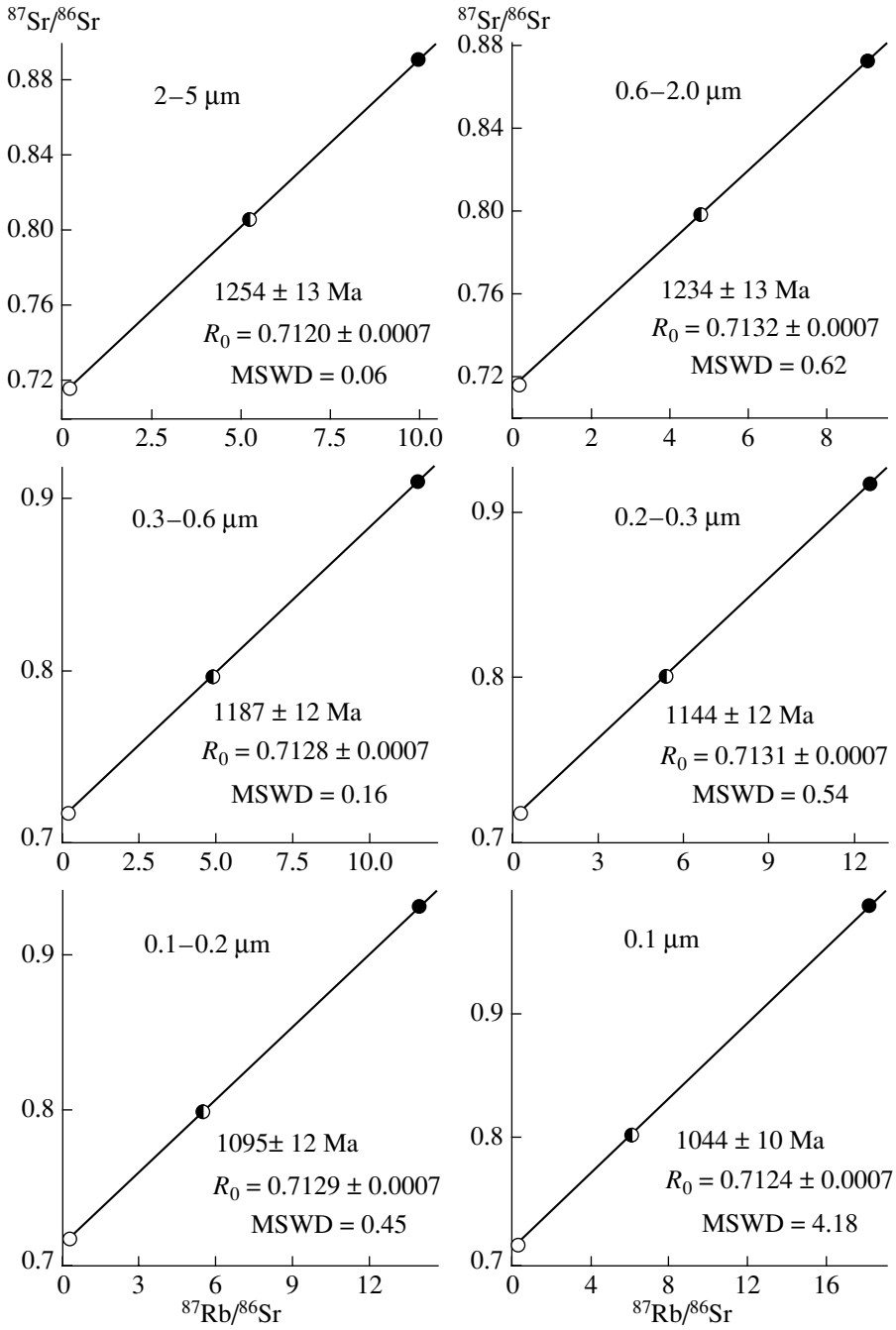

Fig. 9. Inner Rb–Sr isochrons plotted for untreated subfractions, acetate leachates and residues after leaching, Sample 550/2 (symbols as in Fig. 8).

above recrystallization. Consequently, distribution of oxygen and hydrogen isotopes in coarse- and fine-grained SFs of Sample 550/9 discards the possibility of one-stage illite formation in the Debengda shales. The other factors should be responsible in this case for observable variations in isotopic parameters of the SFs, e.g., variations in the environment temperature, composition of diagenetic fluids or water/rock ratio in the course of formation of illite polytypes. Naturally, it is clear that none of these distinctions can take place during the one-stage formation of whole illite material in the shales.

Thus, linear regressions in Figs. 4 and 5 should be interpreted as lines of two-component mixing. This conclusion appears to be correct despite the hypnotizing concordance of the Rb–Sr and K–Ar dates calculated by assumption that these linear regressions have geochronological meaning. In other words, we arrive at

the conclusion that the studied SFs of the Debengda shales include the mixture of low-temperature authigenic illite of two generations. Illite of the first generation (polytype $1M_d$), which is relatively depleted in K and reveals low K/Rb and Rb/Sr ratios but higher $\delta^{18}O$ and δD values, prevails in the coarse-grained SFs (2–5 and 0.6–2 μm). The second generation (polytype 1M–$1M_d$), typical of which are higher K content, high K/Rb and Rb/Sr ratios and relative enrichment in light oxygen and hydrogen isotopes, is most concentrated in the SFs <0.1 μm.

It is essential as well that data points of acetate leachates (discarding those of coarsest and finest SFs) form linear trends in the $^{87}Rb/^{86}Sr$ – $^{87}Sr/^{86}Sr$ diagram (Fig. 7). These trends are characteristic of the other Upper Proterozoic shales (Gorokhov et al., 2001a, 2001b, 2002) and suggest that non-silicate material removed by ammonium acetate from clay fractions also involves two non-cogenetic components of different chemical and isotopic composition. If these mobile components are cogenetic in pairs with two illite generations, the Rb–Sr age of the latter can be calculated by the "inner isochron" method (Gorokhov et al., 2003, 2005).

Applying this method, we estimated the Rb–Sr ages (Figs. 8 and 9), which decline gradually from 1254–1272 (coarsest SFs) to 1038–1044 Ma (finest SFs), while the K–Ar ages simultaneously decrease from 1225–1240 to 1080 Ma (Table 3). It is important therewith that the apparent K–Ar and Rb–Sr ages calculated for the SFs of the same size ranges (Table 3; Figs. 8 and 9) are close to each other. This fact hardly explainable in terms of one-stage catagenetic origin of illite is undoubtedly consistent with the mixing model. Only the *end members* of the mixing, i.e., the coarsest and finest SFs from two samples, are suitable for dating the relevant illite generations. The SFs composed of particles intermediate in size (from 0.1 to 0.6 μm) represent mixtures of minerals different in age, and that is why their Rb–Sr and K–Ar apparent ages have no geochronological meaning.

The $^{87}Sr/^{86}Sr$ initial ratios for both samples characterizing composition of dia- or catagenetic fluids, which controlled formation of two illite generations (Figs. 8 and 9), range from 0.7120 to 0.7143. These values are much greater than the relevant ratio in the Middle Riphean seawater (0.7049–0.7055; Gorokhov et al., 1995b; Semikhatov et al., 2002) and suggest that the fluids were enriched in radiogenic ^{87}Sr because of dissolution of siliciclastic material during the burial of sediments.

The Rb–Sr and K–Ar ages of the SFs 2–5 and 0.6–2 μm, which are composed predominantly of the first illite generation (polytype $1M_d$), range from 1211 to 1272 Ma. They are close to respective dates 1262 ± 13 and 1287 ± 16 Ma obtained for the Debengda glauconites lacking signs of post-diagenetic impact on their structure and isotopic systems, as is inferred from Mössbauer spectra (Gorokhov et al., 1995a; Zaitseva et al., 2004). Since glauconites have been sampled from lower horizons of the Debengda Formation, the minor difference between two sets of dates may reflect either a real distinction of the stratigraphic levels sampled, or the earlier origin of diagenetic glauconite with respect to the first illite generation that originated during the burial catagenesis what is more probable. The other indications of the burial catagenesis have been established in siliciclastic rocks and carbonates of the formation. In particular, these are mosaic, microstylolite to scalloped-microstylolite structures or authigenic quartz and feldspar characteristic of carbonate rocks, as well as a peculiar association of dioctahedral illite changeable in composition and trioctahedral chlorite (Ivanovskaya, 1994; Gorokhov et al., 1995a). Consequently, our results of isotopic-geochronological study are well consistent with stratigraphic age of the Debengda Formation and suggest that the burial diagenesis has not been separated by a considerable time span from diagenesis of sediments that took place soon after their deposition. Similar conclusions have been obtained earlier based on the Rb–Sr systematics of blue clays in northern Estonia (Gorokhov et al., 1994), Upper Riphean shales of the Inzer Formation in the southern Urals (Gorokhov et al., 1995), and Lower Riphean shales of the Ust-Il'ya Formation in the Anabar massif (Gorokhov et al., 1997).

The Rb–Sr and K–Ar ages of 1038 to 1080 Ma established for the second illite generation (SF <0.1 μm, polytype 1M–$1M_d$) correspond to a later stage of lithogenesis. The younger 1M–$1M_d$ illite likely originated during the retrograde catagenesis at the time of the pre-Khaipakh crustal emergence, when the Debengda deposits rose up to the influence zone of meteoric and ground waters. This inference seems reasonable, because the formation time of the second illite generation is concurrent to the pre-Khaipakh hiatus (Shpunt et al., 1979, 1982) and weathering of the Debengda Formation top. Shales of the third subformation studied in this work have been sampled approximately 300 m below the pre-Khaipakh unconformity, and the K–Ar age of glauconites from the Khaipakh Formation base is 1000–960 Ma (*Geochronology…*, 1968). External features indicative of the retrogressive catagenesis are the slight ferrugination of the Debengda Formation rocks and calcitization of some siliciclastic interlayers (Gorokhov et al., 1995a).

CONCLUSIONS

Data considered above lead to the following conclusions:

(1) Shales from the third subformation of the Middle Riphean Debengda Formation contain two authigenic illite polytypes, which are different in age, chemical composition, and the Rb–Sr, K–Ar, O- and H-isotopic systematics.

(2) Both illite generations originated in environments with $^{87}Sr/^{86}Sr$ ratio that was much higher than that in the Middle–early Late Riphean seawater.

(3) According to Rb–Sr and K–Ar ages, the older $1M_d$ illite prevailing in coarse-grained clay subfractions (0.6–2 and 2–5 μm) was formed 1211–1272 Ma ago at the time of burial catagenesis of the Debengda Formation sediments. Consequently, shales of the formation contain authigenic components suitable to determine age approaching the deposition time of sediments.

(4) The Rb–Sr and K–Ar ages of younger $1M–1M_d$ illite concentrated in the finest clay subfractions (<0.1 μm) correspond to 1038–1080 Ma, and this illite likely originated during the retrogressive catagenesis at the time of the pre-Khaipakh break in sedimentation and crustal upwarping in the region.

(5) In the $^{87}Rb/^{86}Sr – ^{87}Sr/^{86}Sr$ and $K–^{40}Ar$ diagrams, pseudoisochrons approximating data points of clay subfractions of different size from the Debengda shales yield formally concordant Rb–Sr and K–Ar ages. Nevertheless, these linear regressions have no geochronological meaning and represent mixing lines of two-component systems.

ACKNOWLEDGMENTS

We are grateful to G.V. Kotov for microphographs of clay particles shot under electron microscope and to A.B. Kuznetsov for his assistance in graphic works. The work was stimulated by research programs of Presidium and Geoscience Division RAS: "Problem of the Origin and Evolution of Biosphere" and "Isotopic Geology, Geochronology and Substance Sources," being simultaneously supported by the Russian Foundation for Basic Research, project nos. 02-05-64210, 02-05-64333, 05-05-64298, and 05-05-65290.

Reviewers Yu.D. Pushkarev and E.V. Bibikova

REFERENCES

1. J. L. Aronson and J. Hower, "Mechanisms of Burial Metamorphism of Argillaceous Sediment. 2. Radiogenic Argon Evidence," Geol. Soc. Am. Bull. **87** (5), 738–744 (1976).
2. J. Bigeleisen, M. L. Perlman, and H. C. Prosser, "Conversion of Hydrogenic Materials to Hydrogen for Isotopic Analysis," Anal. Chem. **25** (12), 1356–1357 (1952).
3. M. G. Bonhomme, "The Use of Rb–Sr and K–Ar Methods as a Stratigraphic Tool Applied to Sedimentary Rocks and Minerals," Precambrian Res. **18** (1/2), 5–25 (1982).
4. M. G. Bonhomme, "Type of Sampling and Comparison Between K–Ar and Rb–Sr Isotopic Dating of Fine Fractions from Sediments in Attempt to Date Young Diagenetic Events," Chem. Geol. **65** (3/4), 209–222 (1987).
5. S. A. Bowring, J. P. Grotzinger, C. E. Isachsen, et al., "Calibration Rates of Early Cambrian Evolution," Science **261** (5126), 1293–1298 (1993).
6. R. H. Brigham and J. R. O' Neil, "Genesis and Evolution of Water in a Two-Mica Pluton: A Hydrogen Isotope Study," Chem. Geol. **48** (1/3), 159–177 (1985).
7. N. Clauer, *Géochimie isotopique du strontium des milieux sédimentaires. Application a la géochronologie de la couverture du craton Ouest-Africain*. Sci. Géol. Mém. Strasbourg, No. 45, 1–256 (1976).
8. N. Clauer and S. Chaudhuri, *Clays in Crustal Environments: Isotope Dating and Tracing* (Springer, Berlin, 1995).
9. D. D. Eberl, J. Srodon, M. Kralik, et al., "Ostwald Ripening of Clays and Metamorphic Minerals," Science **248** (4954), 474–477 (1990).
10. J. Esquevin, "Influence de la composition chimique des illites sur leur cristallinité," Bull. Centre Rech. Pau-SNPA **3** (1), 147–153 (1969).
11. A. E. Fallick, C. I. Macaulay, and R. S. Haszeldine, "Implications of Linearly Correlated Oxygen and Hydrogen Isotopic Compositions for Kaolinite and Illite in the Magnus Sandstone, North Sea," Clays Clay Minerals **41** (2), 184–190 (1993).
12. *Geochronology of Precambrian in the Siberian Platform and Flanking Fold Structures* (Nauka, Leningrad, 1968), p. 332 [in Russian].
13. I. M. Gorokhov and M. A. Semikhatov, "Behavior of Rb and Sr during Sedimentogenesis. Communication 2. Behavior of Rb and Sr during Diagenesis, Catagenesis and Incipient Metamorphism," Litol. Polezn. Iskop., No. 2, 87–109 (1984).
14. I. M. Gorokhov, N. Clauer, T. L. Turchenko, et al., "Rb–Sr Systematics of Vendian-Cambrian Claystones from the East European Platform: Implications for a Multi-Stage Illite Evolution," Chem. Geol. **112** (1/2), 71–89 (1994).
15. I. M. Gorokhov, S. B. Felitsyn, T. L. Turchenko, et al., "Mineralogy, Geochemistry and Isotopic Geochronology of Upper Vendian Shales from the Moscow Syneclise," Stratigr. Geol. Korrelyatsiya **13** (5), 21–41 (2005) [Stratigr. Geol. Correlation **13** (5), 476–494 (2005)].
16. I. M. Gorokhov, N. N. Mel'nikov, V. Z. Negrutsa, et al., "The Multistage Illite Evolution in Upper Proterozoic Claystones from the Srednii Peninsula, Murmansk Coast of the Barents Sea," Litol. Polezn. Iskop., No. 2, 188–207 (2002) [Lithol. Miner. Resour. **37** (2), 162–179 (2002)].
17. I. M. Gorokhov, N. N. Mel'nikov, T. L. Turchenko, and E. P. Kutyavin, "Rb-Sr Systematics of Pelitic Fractions in Lower Riphean Claystones: Ust'-Ilya Formation, Anabar Massif, Northern Siberia," Litol. Polezn. Iskop., No. 5, 530–539 (1997) [Lithol. Miner. Resour. **32** (5), 463–471 (1997)].
18. I. M. Gorokhov, N. N. Melnikov, T. L. Turchenko, et al., "Two Illite Generations in an Upper Riphean Shale: The Rb-Sr Isotopic Evidence," in *EUG 8, Strasbourg, France, 9-13 April*, Terra Abstracts **7**, 330–331 (1995).
19. I. M. Gorokhov, M. A. Semikhatov, A. V. Baskakov, et al., "Sr Isotopic Composition in Riphean, Vendian, and Lower Cambrian Carbonates from Siberia," Stratigr. Geol. Korrelyatsiya **3** (1), 3–33 (1995b) [Stratigr. Geol. Correlation **3** (1), 1–28 (1995b)].

20. I. M. Gorokhov, M. A. Semikhatov, E. R. Drubetskoi, et al., "Rb–Sr and K–Ar Ages of Sedimentary Geochronometers from the Lower Riphean of the Anabar Massif," Izv. Akad. Nauk SSSR, Ser. Geol., No. 7, 17–32 (1991).

21. I. M. Gorokhov, M. A. Semikhatov, and N. N. Mel'nikov, "Once More about the Rb–Sr Isochron Method of Dating the Sedimentary Rocks," Stratigr. Geol. Korrelyatsiya **11** (6), 122–135 (2003) [Stratigr. Geol. Correlation **11** (6), 642–652 (2003)].

22. I. M. Gorokhov, M. A. Semikhatov, N. N. Mel'nikov, et al., "Rb–Sr Geochronology of the Middle Riphean Shale, the Yusmastakh Formation of the Anabar Massif, Northern Siberia," Stratigr. Geol. Korrelyatsiya **9** (3), 3–24 (2001) [Stratigr. Geol. Correlation **9** (3), 213–231 (2001)].

23. I. M. Gorokhov, A. Siedlecka, D. Roberts, et al., "Rb–Sr Dating of Diagenetic Illite in Neoproterozoic Shales, Varanger Peninsula, Northern Norway," Geol. Mag. **138** (5), 541–562 (2001).

24. I. M. Gorokhov, O. V. Yakovleva, M. A. Semikhatov, and T. A. Ivanovskaya, "Rb–Sr and K–Ar Ages and Mössbauer Spectra of Globular Phyllosilicates of Glauconite Series: The Middle Riphean Debengda Formation of the Olenek Uplift, North Siberia," Litol. Polezn. Iskop., No. 6, 615–631 (1995a) [Lithol. Miner. Resour. **30** (5), 556–571 (1995)].

25. C. T. Harper, "Graphical Solutions to the Problem of Radiogenic Argon-40 Loss from Metamorphic Minerals," Eclogae Geol. Helv. **63** (1), 119–140 (1970).

26. J. M. Hayes, Y. R. Kaplan, and K. W. Wedeking, "Precambrian Organic Geochemistry: Preservation and Record," in *Earth's Earliest Biosphere* (Princeton Univ. Press, Princeton, 1983), pp. 93–134.

27. J. Hoefs, *Stable Isotope Geochemistry*, 2nd ed. (Springer, Berlin, 1980; Mir, Moscow, 1983).

28. H. F. Hofmann, "Proterozoic and Selected Cambrian Megascopic Carbonaceous Films." in *The Proterozoic Biosphere. A Multidisciplinary Study* (Cambridge Univ. Press, Cambridge, 1992), pp. 957–979.

29. A. W. Hofmann, J. W. Mahoney, and B. Giletti, "K–Ar and Rb–Sr Data on Detrital and Post-Depositional History of Pennsylvanian Clay from Ohio and Pennsylvania," Bull. Geol. Soc. Am. **85** (4), 639–644 (1974).

30. J. Hower, P. M. Hurley, W. H. Pinson, and H. W. Fairbairn, "The Dependence of K–Ar Age on the Mineralogy of Various Particle Size Ranges of Shale," Geochim. Cosmochim. Acta **27** (4), 405–410 (1963).

31. P. M. Hurley, J. M. Hunt, W. H. Pinson, and H. W. Fairbairn, "K–Ar Age Values on the Clay Fractions in Dated Shales," Geochim. Cosmochim. Acta **27** (2), 279–284 (1963).

32. T. A. Ivanovskaya, "Globular Layered Silicates of Glauconite–Illite Composition from the Debengda Formation Rocks (Middle Riphean of the Olenek Uplift)," Litol. Polezn. Iskop., No. 6, 101–113 (1994).

33. G. A. Kazakov, K. G. Knorre, and L. N. Prokof'eva, "Absolute Age of Precambrian Sedimentary Rocks in the Olenek Uplift, East Siberia," Geokhimiya, No. 11, 1313–1317 (1965).

34. V. V. Khomentovskii, "The Event Basis of Neoproterozoic Stratigraphic Scale in Siberia and China," Geol. Geofiz. **37** (8), 43–56 (1996).

35. V. V. Khomentovskii and G. A. Karlova, "The Boundary between Nemakit-Daldynian and Tommotian Stages (Vendian–Cambrian Systems) of Siberia," Stratigr. Geol. Korrelyatsiya **10** (3), 13–34 (2002) [Stratigr. Geol. Correlation **10** (3), 217–238 (2002)].

36. V. V. Khomentovskii, V. Yu. Shenfil', and M. S. Yakshin, "The Riphean of Siberian Platform," Geol. Geofiz., No. 7, 25–33 (1985).

37. H. J. Kisch, "Incipient Metamorphism of Cambro-Silurian Clastic Rocks from the Jamtland Supergroup, Central Scandinavian Caledonides, Western Sweden: Illite Crystallinity and 'Vitrinite' Reflectance," J. Geol. Soc. (London) **137** (3), 271–288 (1980)

38. V. A. Komar, *Stromatolites from Upper Precambrian Deposits of the North Siberian Platform and Their Stratigraphic Significance* (Nauka, Moscow, 1966) [in Russian].

39. B. Kubler, "La cristallinité de l'illite et les zones tout à fait supérieures du métamorphisme," in *Colloque sur lés etages tectoniques, Univ. Neuchatel*, Ed. by J.-P. Schaer (Baconniere, Neuchatel, 1966), pp. 105–122.

40. B. Kubler, "Cristallinité de l'illite et mixed-layers: brève révision," Schweiz. Mineral. Petrogr. Mitt. **70** (1), 89–93 (1990).

41. Y. Kuroda, T. Suzuoki, S. Matsuo, and H. Shirozu, "A Preliminary Study of D/H Ratios of Chlorites," Contrib. Mineral. Petrol. **57** (2), 223–225 (1976).

42. J. R. Lawrence and H. P. Taylor, "Hydrogen and Oxygen Isotope Systematics in Weathering Profiles," Geochim. Cosmochim. Acta **36** (12), 1377–1393 (1972).

43. C. I. Macaulay, A. E. Fallick, R. S. Haszeldine, and C. M. Graham, "Methods of Laser-Based Stable Isotope Measurement Applied to Diagenetic Cements and Hydrocarbon Reservoir Quality," Clay Miner. **35**, 313–322 (2000).

44. G. A. McIntyre, C. Brooks, W. Compston, and A. Turek, "The Statistical Assessment of Rb–Sr Isochrons," J. Geophys. Res. **71** (22), 5459–5468 (1966).

45. N. N. Mel'nikov, I. M. Gorokhov, T. L. Turchenko, et al., "Mineralogical and Isotopic Study of Fine-Grained Fraction from Upper Precambrian Clay Rocks of the Podol Area near Dniester and Southern Urals," in *Isotopic Geochemistry and Geochronology* (Nauka, Leningrad, 1990), pp. 85–97 [in Russian].

46. J. P. Morton, "Rb–Sr Evidence for Punctuated Illite/Smectite Diagenesis in the Oligocene Frio Formation, Texas Gulf Coast," Geol. Soc. Amer. Bull. **96** (1), 114–122 (1985a).

47. J. P. Morton, "Rb–Sr Dating of Diagenesis and Source Age of Clays in Upper Devonian Black Shales of Texas," Geol. Soc. Amer. Bull. **96** (8), 1043–1049 (1985b).

48. V. A. Ponomarchuk, V. Yu. Shenfil', M. S. Yakshin, et al., "A Direct K–Ar Dating of Stromatolites from the Olenek Uplift," Dokl. Akad. Nauk **339** (3), 378–381 (1994).

49. M. A. Semikhatov, "Stromatolites in Precambrian Stratigraphy: Analysis 84," Izv. Akad. Nauk SSSR, Ser. Geol., No. 4, 3–21 (1985).

50. M. A. Semikhatov, "Verified Base Ages of the Upper Riphean, Vendian, Upper Vendian and Lower Cambrian," in *Addenda to the Stratigraphic Code of Russia* (VSEGEI, St. Petersburg, 2000), pp. 95–107 [in Russian].

51. M. A. Semikhatov and S. N. Serebryakov, *The Riphean Hypostratotype of Siberia* (Nauka, Moscow, 1983) [in Russian].

52. M. A. Semikhatov, A. B. Kuznetsov, I. M. Gorokhov, et al., "Low $^{87}Sr/^{86}Sr$ Ratios in Seawater of the Grenville and post-Grenville Time: Determining Factors," Stratigr. Geol. Korrelyatsiya **10** (1), 3–46 (2002) [Stratigr. Geol. Correlation **10** (1), 1–41 (2002)].

53. M. A. Semikhatov, A. B. Kuznetsov, V. N. Podkovyrov, et al., "The Yudoma Group of Stratotype Area: C-isotope Chemostratigraphic Correlations and Yudomian-Vendian Relation," Stratigr. Geol. Korrelyatsiya **12** (5), 3–28 (2004) [Stratigr. Geol. Correlation **12** (5), 435–459 (2004)].

54. M. A. Semikhatov, K. A. Shurkin, E. M. Aksenov, et al., "The New Precambrian Stratigraphic Scale of the USSR," Izv. Akad. Nauk SSSR, Ser. Geol., No. 4, 3–13 (1991).

55. V. N. Sergeev, A. H. Knoll, S. P. Kolosova, and P. N. Kolosov, "Microfossils in Cherts from the Mesoproterozoic (Middle Riphean) Debengda Formation, the Olenek Uplift, Northeastern Siberia," Stratigr. Geol. Korrelyatsiya **2** (1), 23–38 (1994) [Stratigr. Geol. Correlation **2** (1), 19–33 (1994)].

56. Z. D. Sharp, "A Laser-Based Microanalytical Method for the in Situ Determination of Oxygen Isotope Ratios of Silicates and Oxides," Geochim. Cosmochim. Acta **54** (5), 1353–1357 (1990).

57. V. Yu. Shenfil', *Late Precambrian of Siberian Platform* (Nauka, Novosibirsk, 1991) [in Russian].

58. V. Yu. Shenfil', M. S. Yakshin, A. G. Kats, and Z. B. Florova, "Detailing the Upper Part of the Riphean Succession in the Olenek Uplift," in *Late Precambrian and Early Paleozoic of Siberia: Riphean and Vendian* (IGiG SO AN SSSR, Novosibirsk, 1988), pp. 20–36 [in Russian].

59. S. M. F. Sheppard and H. A. Gilg, "Stable Isotope Geochemistry of Clay Minerals," Clay Miner. **31** (1), 1–24 (1996).

60. B. R. Shpunt, I. G. Shapovalova, E. A. Shamshina, et al., *The Proterozoic in Northeastern Margin of Siberian Platform* (Nauka, Novosibirsk, 1979) [in Russian].

61. B. R. Shpunt, I. G. Shapovalova, and E. A. Shamshina, *Late Precambrian in the North Siberian Platform* (Nauka, Novosibirsk, 1982) [in Russian].

62. J. Środoń and D. D. Eberl, "Illite," Rev. Mineral. **13**, 495–544 (1984).

63. T. Suzuoki and S. Epstein, "Hydrogen Isotope Fractionation Between OH-Bearing Minerals and Water," Geochim. Cosmochim. Acta **40** (10), 1229–1240 (1976).

64. H. P. Taylor and S. Epstein, "Deuterium-Hydrogen Ratios in Coexisting Minerals of Metamorphic and Igneous Rocks," Trans. Am. Geophys. Union **47** (1), 213 (1966).

65. G. Vidal, M. Moczydlowska, and V. A. Rudavskaya, "Biostratigraphic Implications of a *Chuaria-Tawuia* Assemblage and Associated Acritarchs from the Neoproterozoic of Yakutia," Paleontology **36**, Part 2, 387–401 (1993).

66. J. H. Williamson, "Least-Squares Fitting of a Straight Line," Can. J. Phys. **46** (16), 1845–1847 (1968).

67. T. S. Zaitseva, I. M. Gorokhov, N. N. Mel'nikov, and O. V. Yakovleva, "Cations Surrounding Fe^{+3} and Fe^{+2} in Octahedral Layers of Glauconite: Models and Data of Mössbauer Spectroscopy," in *Proceedings of the XV International Conference "Geology and Geoecology of European Russia and Adjacent Countries" in Commemoration of K.O.Kratz, October 13–16, 2004, St. Petersburg* (IGGD RAN, St. Petersburg, 2004), pp. 81–82 [in Russian].

68. X. Zhang, "The Relationship Between K–Ar Ages and Grain Size in Middle and Upper Proterozoic Shales from the Yanshan Area, North China," Precambrian Res. **29** (1/3), 175–181 (1985).